



# Role of a ductile décollement in the development of pull-apart basins: Experimental results and natural examples

Darrell Sims, David A. Ferrill\*, John A. Stamatakos

*Center for Nuclear Waste Regulatory Analyses, Southwest Research Institute, San Antonio, TX 78238, USA*

Received 12 January 1998; accepted 8 December 1998

## Abstract

Traditional models describe pull-apart basins as graben or half-graben basins with normal or normal-oblique slip master faults, analogous to Death Valley, California. Yet many pull-aparts are characterized by asymmetric basins with strike-slip master faults indicating that not all pull-apart basins conform to the simple Death Valley models. We present analogue modelling results that show developmental sequences and structural styles of pull-aparts are dramatically different when overburden rides over a ductile horizon, and that thickness of the ductile horizon exerts control on basin development. In our models, synthetic and antithetic strike-slip faults control basin geometries, while localized normal faulting and local oblique slip on strike-slip faults accommodate basin subsidence. Faults evolve from initial strike-slip to normal-oblique and normal dip slip to form a system of either isolated sub-basins in the case of thick ductile layers, or coalescing sub-basins in the case of thin ductile layers. These results demonstrate distinct differences between non-ductile and ductile décollement pull apart structures. Basin boundaries dominated by normal faults suggest a décollement within or at the base of a non-ductile layer similar to Death Valley, California. Basin bounding faults dominated by strike-slip and oblique-slip faults indicate basin formation over a ductile layer, similar to the Gulf of Elat (Aqaba) or Gulf of Paria (Venezuela and Trinidad). © 1999 Elsevier Science Ltd. All rights reserved.

## 1. Introduction

Pull-apart basins are extensional depressions that form at releasing bends in strike-slip fault systems (Carey, 1958; Burchfiel and Stewart, 1966). Basin structure is commonly, but not uniformly, a rhomb-shaped graben or half-graben terminated by strike-slip faults (Aydin and Nur, 1985; Price and Cosgrove, 1990). Natural examples include Death, Panamint, and Saline Valleys of the eastern California shear zone (Burchfiel and Stewart, 1966; Burchfiel et al., 1987). Much work has been applied to the interpretation of pull-apart basins, yet the more complicated examples in nature are not easily explained by existing models. The Gulf of Paria (Flinch et al., in press) and the

Cariaco Basin (Ben-Avraham and Zoback, 1992), northeastern Venezuela, and the Gulf of Elat, Dead Sea Rift (Ben-Avraham and Zoback, 1992) are examples where basin symmetry and kinematics depart from the dip-slip dominated graben or half-graben model of pull-apart development. These basins show marked asymmetry with major strike-slip faults serving as basin bounding master faults. The strike-slip faults show a visible normal-slip component and opposite-facing normal faults define the opposing basin margin (Flinch et al., in press).

Analogue modelling has proven a valuable tool in the investigation of both extensional (McClay and Ellis, 1987; Vendeville et al., 1987; Withjack et al., 1995) and strike-slip (Cloos, 1955; Tchalenko, 1970; Richard et al., 1991) deformation, including application to understanding pull-apart basin evolution (Hempton and Neher, 1986; Faugère et al., 1986; McClay and Dooley, 1995; Rahe et al., 1998). Thus

\* Corresponding author.

*E-mail address:* dferrill@swri.edu (D.A. Ferrill)

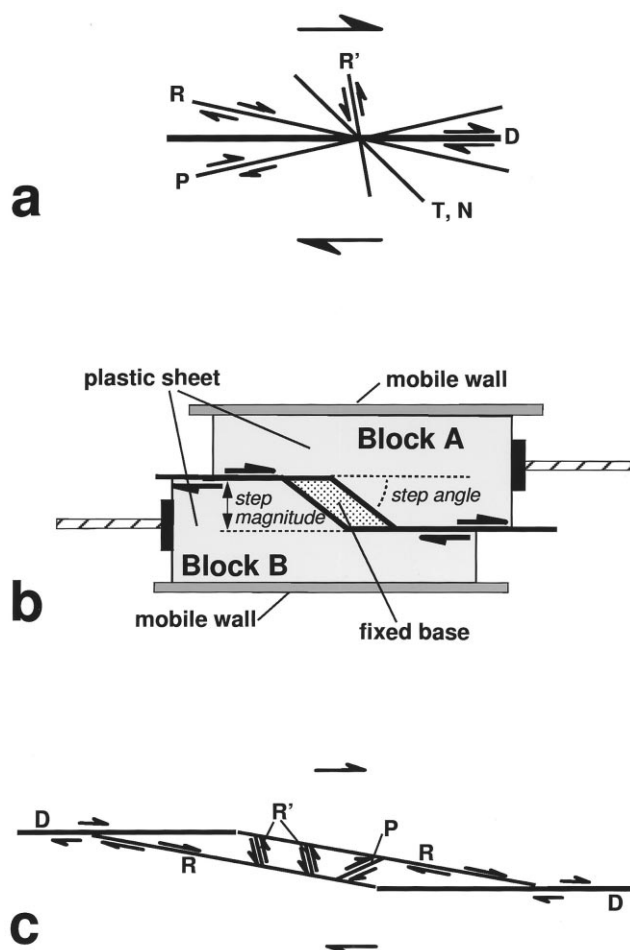


Fig. 1. (a) Structures associated with strike-slip faults and orientations relative to a single main displacement zone (**D**): **R** shears (synthetic Riedel), **R'** shears (antithetic Riedel), **P** shears, **T** tension fractures, and **N** normal faults (modified from Rahe et al., 1998). (b) Plan view of the deformation rig after run is completed. Configuration is a right-stepping jog in en échelon strike-slip faults. (c) Schematic diagram showing relative orientation of structures observed in our models as described in text. **R**, **R'** and **P** shears are distributed between en échelon main displacement zones (**D**).

far, analogue models of pull-apart basins have been confined to single rheology strata over rigid (inflexible) mechanical décollements represented by sliding plates of plastic or metal. In this paper we use the term décollement to describe a shallow-dipping to horizontal fault or shear zone separating deformed material above the décollement from nondeformed material below the décollement (Jackson, 1997). Mechanical décollement refers to rigid or inflexible mobile sheets (in our models plastic drafting film) separating rock analogues resting upon the sheets from a fixed base plate. Hempton and Neher (1986) used monochrome claycake models to examine plan view strain and subsidence patterns over a 2.5 cm thick rigid sliding plate. Vertical displacement was controlled in part by a gap opening in the mechanical décollement, and vertical

profiles were not recovered from the models. Faugère et al. (1986), Horsfield and Naylor (fig. I.4-19c, in Mandl, 1988), McClay and Dooley (1995), Richard et al. (1995), and Rahe et al. (1998) used color-layered dry sand over a thin mechanical décollement (plastic sheet) and recovered profiles from finished models. Results from these models indicate that basin plan-view geometry is controlled, in part, by the amount of offset and over- or underlap of en échelon strike-slip fault segments relative to overburden thickness (Mandl, 1988; Richard et al., 1995). Internal geometries and basin symmetry are controlled by displacement (Faugère et al., 1986) and by relative displacement rates across the strike-slip faults (Rahe et al., 1998). Structural features and geometries of many natural pull-apart basins are replicated in these sandbox models (Hempton and Neher, 1986; McClay and Dooley, 1995; Rahe et al., 1998). These models are particularly valid in cases where basins are interpreted to form as soft-sediment overburden riding passively on rigid basement blocks (McClay and Dooley, 1995). The sandpack-only models do not reflect the influence of ductile décollements observed in many natural systems, and may therefore not accurately represent such systems.

Sandpack pull-apart models with thin rigid décollements show a consistent developmental sequence (Rahe et al., 1998): faulting initiates as **N** shears (normal displacement, see Fig. 1) defining the basin edges, followed closely by **D** (displacement parallel) and **R** (synthetic Riedel) strike-slip shears that define the primary strike-slip fault segments beyond the ends of the basin. With continued displacement, **R** shears develop as cross-basin strike-slip faults that terminate against basin bounding normal faults. Basins reach maturity when a through-going **R** shear develops that extends tip to tip across the basin connecting the primary strike-slip faults. Formation of the through-going strike-slip fault is generally accompanied by basin subsidence concentrating nearer the central axis of the basin and gradually decreasing displacement on normal faults along basin margins. Master faults that define basin symmetry show predominantly normal displacement accommodating extension parallel to the major strike-slip (**D** shears, displacement parallel) faults at and beyond the tips of the basin. Through-going strike-slip or cross-basin faults form later and are concentrated toward the center of the basin. Cross-basin strike-slip faults show limited normal displacement. Formation of cross-basin faults generally marks a reduction in dip-slip rate of the master normal faults in physical models and possibly a general extinction of basin subsidence in nature (Zhang and Burchfiel, 1989).

Evidence from some basins formed at strike-slip releasing bends indicates that strike-slip faults that

transect or bound the basins form early. Elat and Dakar Deeps in the Dead Sea Rift and the Cariaco Basin, offshore northern Venezuela, are basins bound on one side by strike-slip faults with long-lived displacement histories, and by normal faults on the opposing side (Schubert, 1984; Ben-Avraham, 1992; Ben-Avraham and Zoback, 1992). These strike-slip faults serve as master faults of asymmetric basin growth with significant normal displacement. Early forming wrench faults are not observed in single rheology sandpack models of releasing bends and are not expected as the differential stress required to initiate normal faulting is much less than required for strike-slip faulting (Mandl, 1988, pp. 154).

Décollements in some pull-apart basins are observed (ten Brink and Ben-Avraham, 1989) or postulated (Burchfiel et al., 1989) within ductile or viscous zones at depth. Décollement-zone strength affects structural development in most tectonic regimes (Molnar and Lyon-Caen, 1988) and likely exhibits some control on development of pull-aparts. In this study, we use analogue modelling to evaluate deformation in strike-slip releasing bends where brittle rock or sediment (represented by the sandpack) deforms above a ductile décollement zone such as the ductile lower crust (represented by silicone putty). We present one sand-pack model constructed without the putty layer as a reference frame for non-ductile décollement models. Model results are then compared against natural examples of strike-slip releasing bends from the eastern California shear zone, the Gulf of Elat (Aqaba), and the Gulf of Paria (Venezuela and Trinidad). The results demonstrate strong similarities between models and natural examples and indicate that deformation in strike-slip releasing bends is sensitive to décollement zone rheology.

## 2. Methods

We test the effects of a viscous substrate on pull-apart development using physical analogue models (summarized in Table 1). The models are scaled (Table 2) in the manner of Hubbert (1937) and Ramberg (1967) and are initially composed of a 5 cm thick sandpack of alternating acrylic dyed and plain white layers (pre-kinematic, commercially named Oklahoma #1) resting over a constant-thickness putty layer on a mobile plastic sheet. The whole model package rides over a fixed horizontal metal base (Fig. 1). The model representing a décollement in non-ductile rock is similarly constructed, but the constant thickness putty layer is omitted (model 7, Table 1). The plastic sheet serves as a horizontal mechanical décollement and is cut to form a 40° right-stepping jog in a right-lateral strike-slip fault in the fashion of Rahe et al. (1998). In each experiment except model 9 (Tables 1 and 2), the stepover magnitude is 16.2 cm measured normal to the strike-slip fault. In the case of model 9 (26Jul96), the stepover magnitude is 10 cm and left-stepping. Constant thickness model dimensions are 90 cm × 50 cm in plan view. The long edges (parallel to strike-slip displacement direction) of the model rest against mobile walls and the whole model rests on and moves in concert with the plastic sheet. To reduce boundary effects produced by rigid mobile walls indenting the model, walls are not employed along the short ends (normal to strike-slip displacement direction); rather, the sandpack is allowed to spill at repose angle over the edge of the putty layer. Constant velocity is imparted by stepper motors that drive the mobile walls and plastic mechanical décollement (Fig. 1b). The upper surface of the sandpack is marked with a passive grid, and dyed sand is added as syn-deformational fill (syn-kinematic layers) to better preserve fault scarps

Table 1  
Model dimensions and displacement parameters

#	Model	Putty thickness (cm)	Step magnitude (cm)	Block A disp. @ rate (cm) @ (cm/h)	Block B disp. @ rate (cm) @ (cm/h)	Displacement and rate ratio B:A
1.	22Aug96	1	16.2	5 @ 5	5 @ 5	1:1
2.	29Aug96	1	16.2	7.5 @ 7.5	2.5 @ 2.5	3:1
3.	15Aug96	1	16.2	10 @ 10	0	10:1
4.	18Sep96	0.5	16.2	5 @ 5	5 @ 5	1:1
5.	31Jul97	0.5	16.2	7.5 @ 7.5	2.5 @ 2.5	3:1
6.	24Sep96	0.5	16.2	10 @ 10	0	10:0
7.	26Sep96	0	16.2	5 @ 5	5 @ 5	1:1
8.	24Jul97	1	16.2	5 @ 5	5 @ 5	1:1
9.	26Jul96	1	10	9 @ 1	0	9:0

Table 2  
Scaling ratios

Model number	Model values	Prototype values	Model ratio
1–6. (see Table 1)			
viscosity (Pa s)	$10^4$	$10^{21}$	$10^{-17}$
density* (g/cm <sup>3</sup> )	1.14	2.85	0.4
length (cm)	1	$2 \times 10^5$	$5 \times 10^{-6}$
time	1 (h)	$2.28 \times 10^7$ (y)	$5 \times 10^{-12}$
strain rate			$2 \times 10^{11}$
7. (26Sep96)			
length (cm)	1	$2 \times 10^5$	$5 \times 10^{-6}$
8. (24Jul97)			
viscosity (Pa s)	$10^5$	$10^{21}$	$10^{-16}$
density* (g/cm <sup>3</sup> )	1.14	2.85	0.4
length (cm)	1	$2 \times 10^5$	$5 \times 10^{-6}$
time	1 (h)	$2.28 \times 10^6$ (y)	$5 \times 10^{-11}$
strain rate			$2 \times 10^{10}$
9. (26Jul96)			
viscosity (Pa s)	$10^4$	$10^{19}$	$10^{-15}$
density* (g/cm <sup>3</sup> )	1.14	2.3	0.5
length (cm)	1	$1.5 \times 10^5$	$6.67 \times 10^{-6}$
time	8 (h)	$3 \times 10^6$ (y)	$3 \times 10^{-10}$
strain rate			$3 \times 10^9$

\* Density values are for ductile elements.

and basin geometries and to simulate basin fill. When the model run is concluded, it is covered with a uniform-thickness layer of plain white sand to protect fault scarps and to ensure that no post-kinematic deformation related to flow of putty occurs. The sandpack is then wetted, serially sliced, and photographed to produce cross-sectional views.

The series of experiments (Table 1) tests the effects of weak-layer thickness and relative and absolute displacement rates. The models are run for one hour for a total strike-slip displacement of 10 cm. Rahe et al. (1998) demonstrated that relative velocity differences of opposing fault blocks control basin symmetry. We test for this effect in our models using relative rates given as ratios of 1:1, 3:1, and 10:0, all at cumulative displacement rates of 10 cm/h. For example, models where the opposing blocks move at 5 cm/h for one hour have a displacement ratio of 1:1; total or cumulative displacement across the primary strike slip faults is 10 cm. Models are constructed with 0.5 cm and 1.0 cm thick putty layers for each displacement ratio. A single model with no putty layer deformed using a 1:1 displacement velocity ratio serves as control.

We designed our models to represent a homogeneous rock sequence separated by a ductile layer from a major strike-slip fault at depth. In our models, the sandpack over the ductile putty layer represents a brittle rock sequence over a ductile substrate. Displacement across the step in the plastic sheet represents the horizontal portion of a listric fault geometry. Our mechanical décollement and fixed base scale to a natural 'basement' of infinite strength and pre-

clude vertical motion of our basal fault. While this is by no means a rheologically accurate representation of the lower crust, the kinematics and displacement gradients produced by the plastic sheet are acceptable for the purpose of scaling strike-slip displacement across a narrow fault zone at depth. Décollements in nature may be in a variety of rock types and at a variety of depths. Rather than attempt to reproduce each possible scenario, we have, for convenience, scaled our models to represent décollements situated in the ductile lower crust. Our models demonstrate distinct differences between non-ductile and ductile décollement pull-apart structures.

### 3. Results

To illustrate pull-apart basin development over a non-ductile décollement, we present a symmetrical pull-apart model with no basal putty layer (Model 26Sep96, Table 1). The developmental sequence for this model was similar to that of Rahe et al. (1998), as described in the introduction of this paper (Figs. 2 and 3). Our symmetric pull-apart basin model reached the mature stage of development described by Rahe et al. (1998) at a similar cumulative displacement (4.0 cm in our model), with subsidence concentrating at the center of the basin, coeval with the development of through-going cross-basin faults. Although similar to the symmetrical pull-apart models described by Rahe et al. (1998), our model geometrically scales to represent twice the total cumulative displacement because

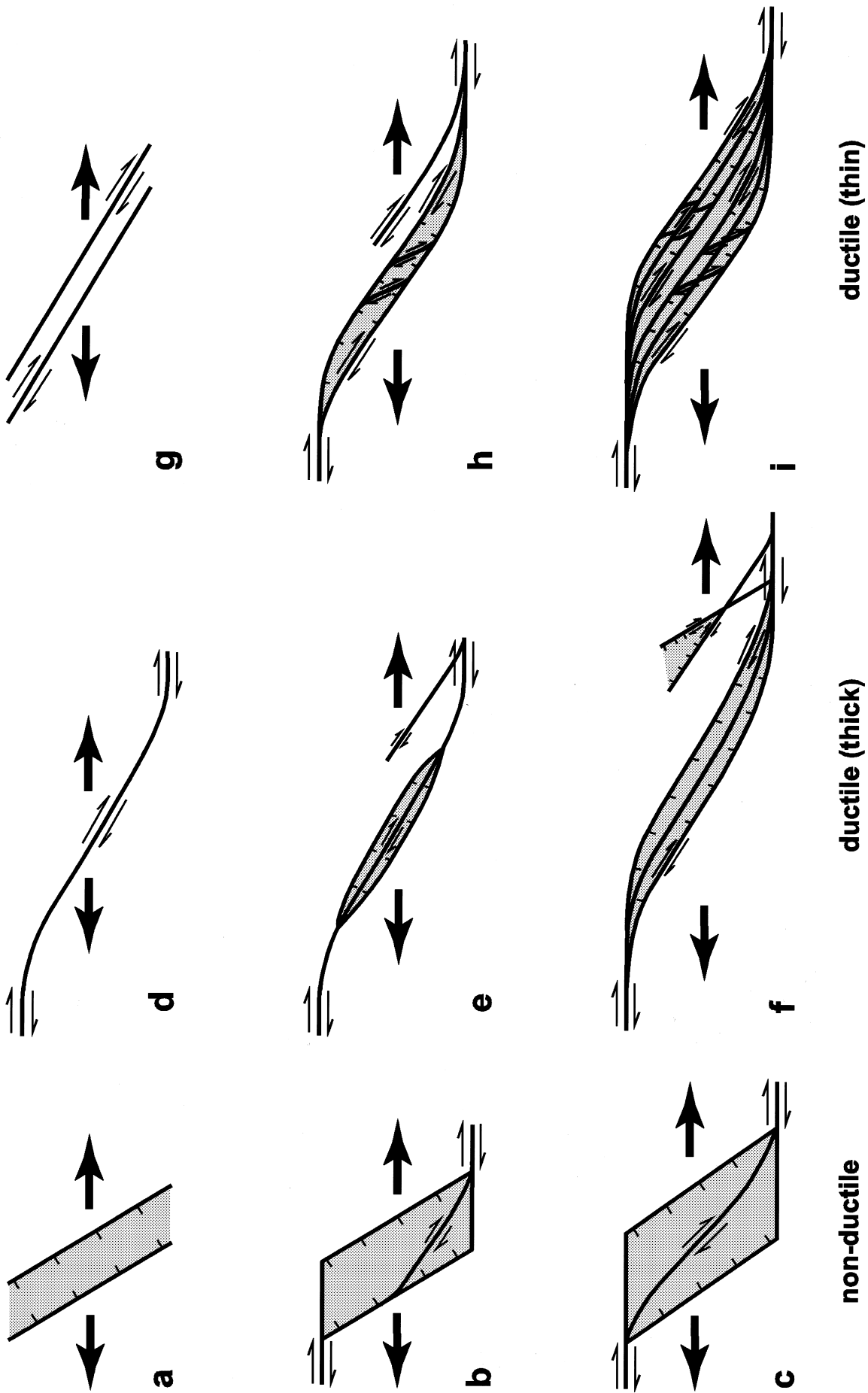


Fig. 2. Schematic plan view of physical analogue pull-apart basin development over non-ductile (a–c), thick ductile (d–f) and thin ductile (g–i) décollements. Areas of subsidence are denoted by shading.

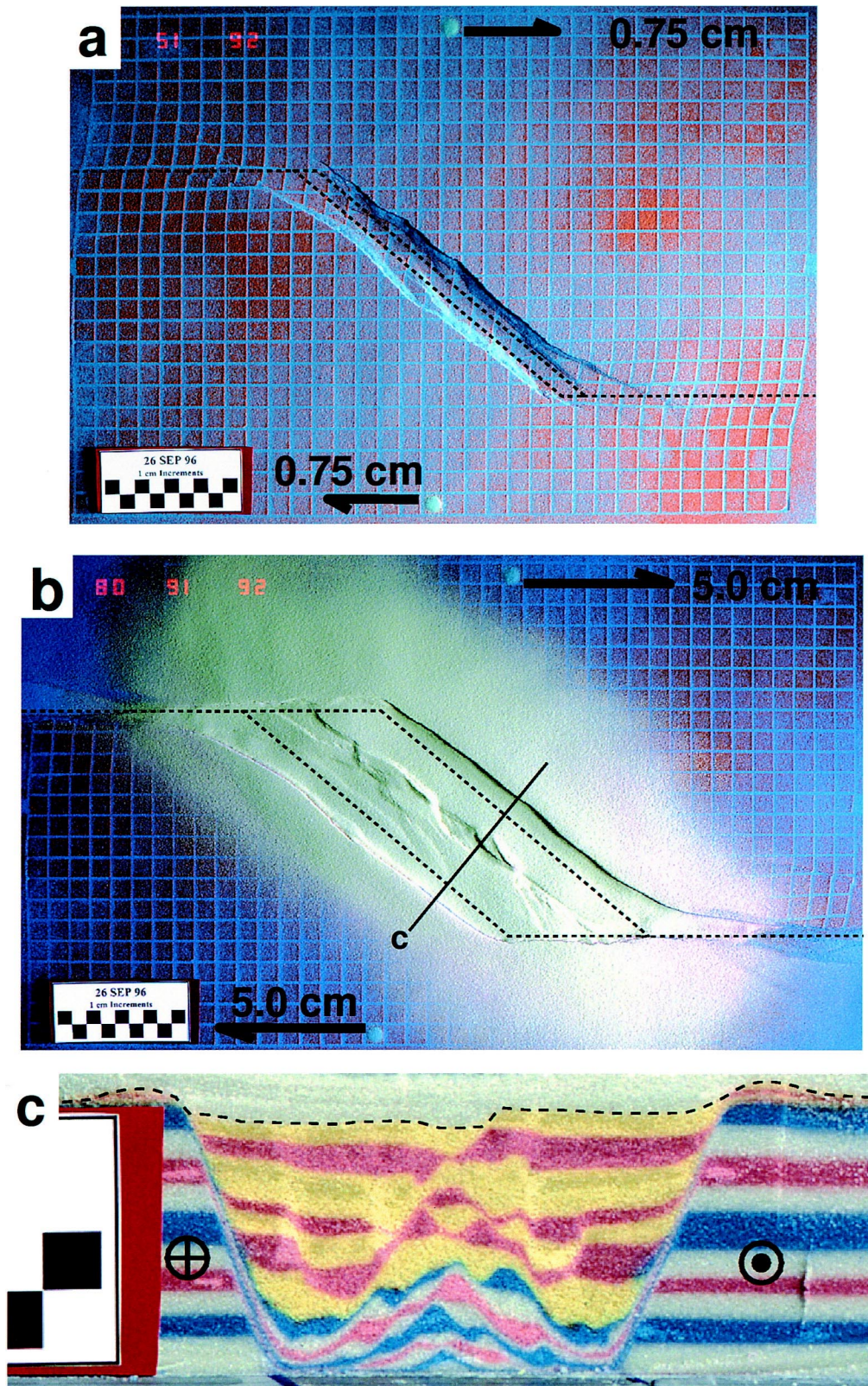


Fig. 3. (a–b) Plan views of pull-apart basin development in physical model without putty substrate (Model 26Sep96). Profile (c) shows symmetrical basin with dissected central horst in pre-kinematic layers. Alternating white, blue, and red layers are pre-kinematic. Alternating yellow and red are syn-kinematic. White layer over all at top separated by thin dashed line is post-kinematic cover. Circle with dot (cross) indicates displacement out-of (into) page. Scale is in centimeters, and upper surface grid is 1.5 cm  $\times$  1.5 cm. Low angle lighting from right. Displacement labelled for upper (A) and lower (B, see Fig. 1b) blocks. Position of mechanical décollement shown as black, thin dashed line. Light-colored sand patches obscuring grid are syn-kinematic layers. Thin solid line shows position of profile (c), and labelled end of profile view corresponds to labelled end of location line.

of differences in sandpack thickness from dimensions of models by Rahe et al. (1998). The increased displacement in our model is most evident in cross-section geometry. In profile view, the symmetric basin is defined by master normal-slip faults with opposing dips. The central basin horst in the pre-kinematic layers is dissected by a complex system of crossing faults that produce grabens in the overlying syn-kinematic layers. In our model, the formation of through-going cross-basin faults did not arrest basin development.

The developmental sequence over a viscous substrate

is markedly different from that observed over a non-ductile décollement. In each case with a viscous décollement (and regardless of décollement thickness), faulting initiates as **R** shears (strike-slip faults, Fig. 1c) oriented subparallel with the right-stepping jog in the plastic sheet (Figs. 2, 4a, 5a and 6a). Formation of the **R** shears is followed closely by antithetic **R'** shears and synthetic **P** shears that link the **R** shears into fault-bounded horses in strike-slip duplexes. The duplexes are observed to rotate dextrally, sympathetic with displacement along the primary strike-slip faults.

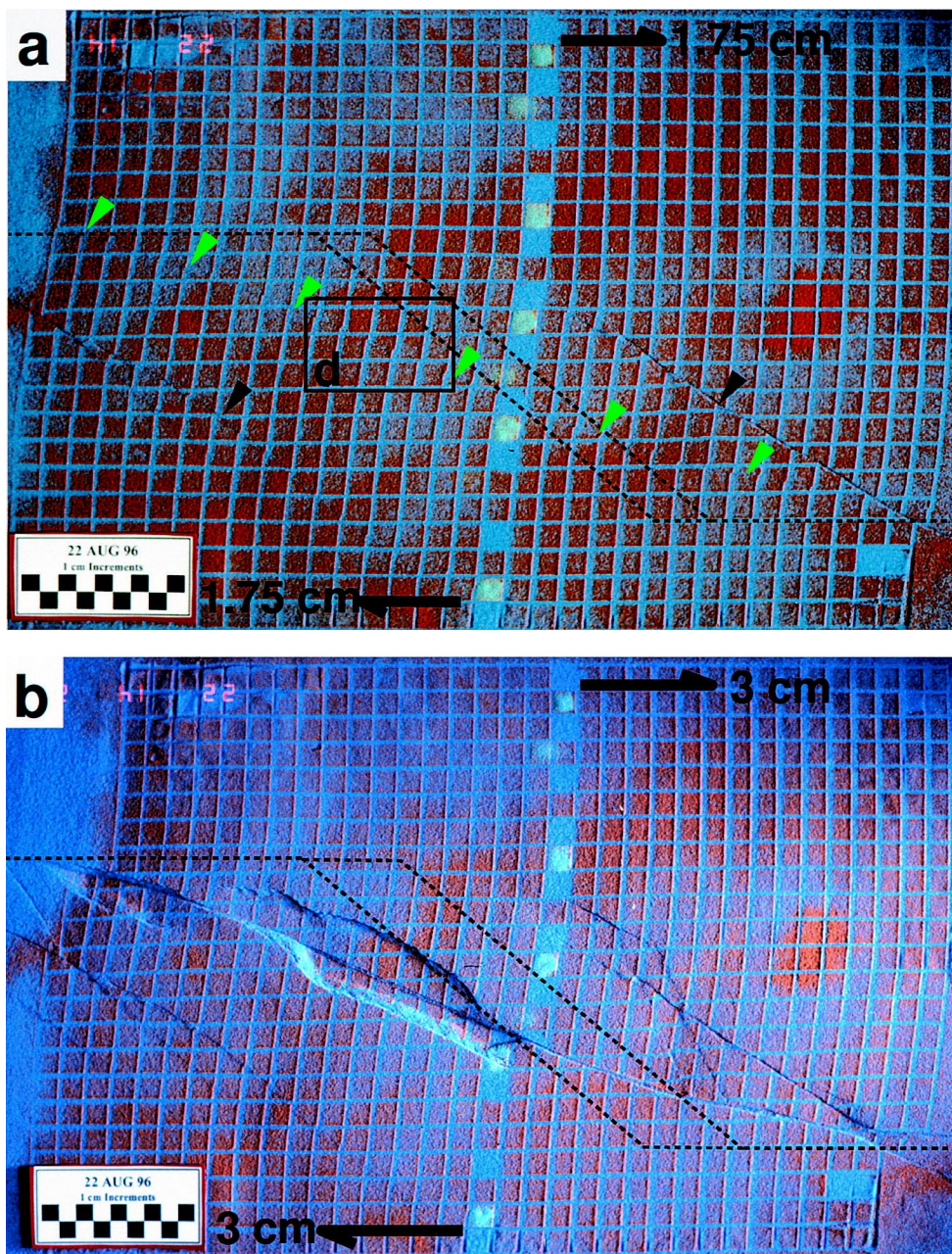


Fig. 4. Photographic map views showing pull-apart basin development over thick (1 cm) putty layer (Model 22Aug96). Green arrows in (a) mark through-going **R** shear with flanking **R** shears marked by black arrows. BBH—between-basin high. Enlarged view of area outlined in (a) is shown in (d). Details are the same as in Fig. 3.

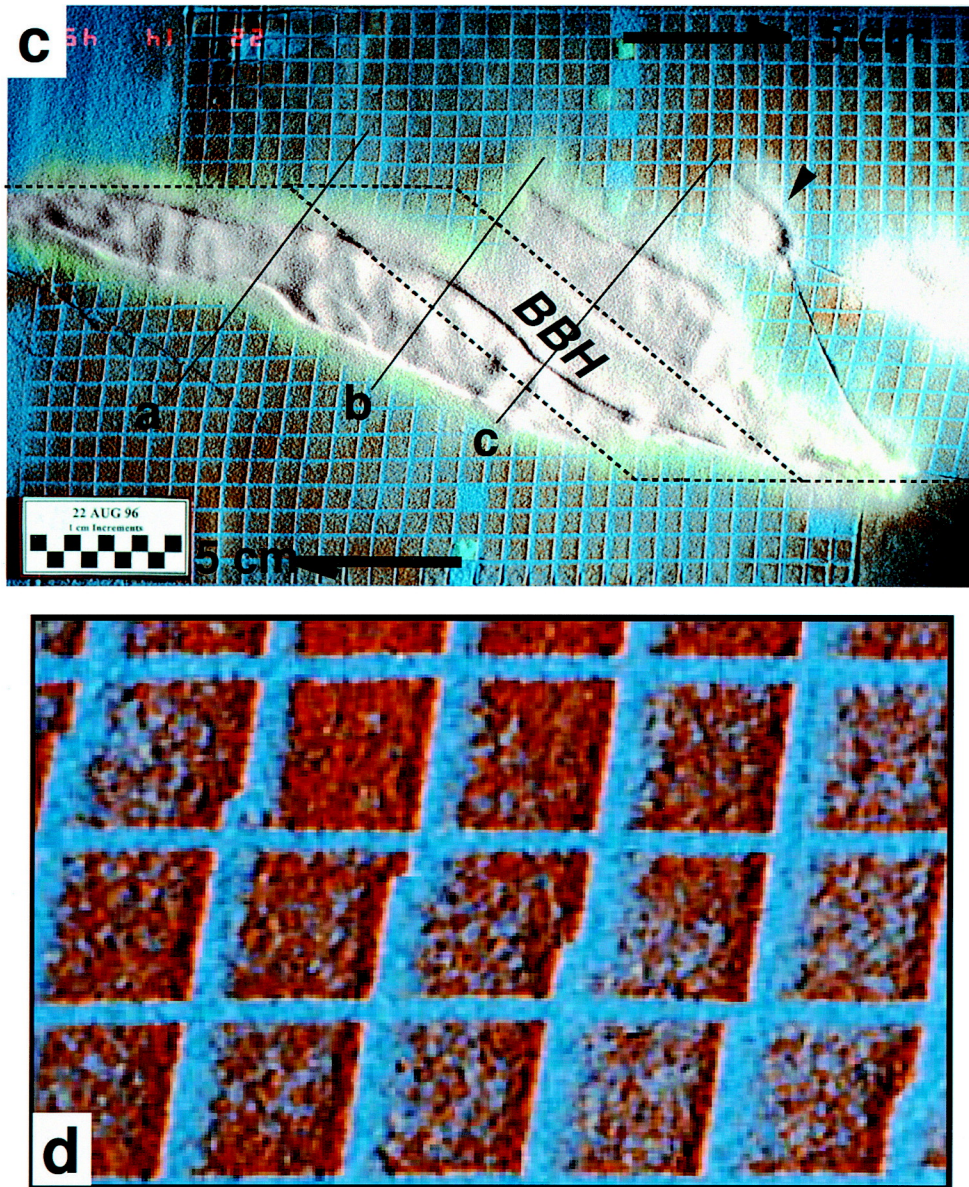


Fig. 4 (continued)

Formation of linear **D** shears, which define the primary strike-slip faults at and beyond the ends of the incipient basins, follows the formation of antithetic **R'** shears.

Basin subsidence (vertical displacement) begins with the formation of localized normal faults, the initiation of localized dip slip on existing **R** and **R'** shears, or both. Normal displacement varies along strike to create asymmetric sub-basins with basin symmetry switching sides along strike. Basin symmetry may be centered along a single major **R** shear (Fig. 4) or between subparallel major **R** shears (Figs. 5 and 6). Large basins are elongate—either bound on one side by a strike-slip fault with normal faults on the opposing side or by a

strike-slip fault flanked on opposing sides by normal or oblique-slip faults. In some cases, active **R** shears develop outside the basin. The amount of vertical displacement along outlying **R** shears may be virtually zero and varies from model to model. In some cases, subsidiary or widely spaced **R** (strike-slip) shears terminate in synthetic oblique-slip **R** and antithetic oblique-slip **R'** shears to form isolated hinged or trapdoor basins (Fig. 4c). The trapdoor basins are bound on all but one side by faults, with the remaining side operating as a hinge.

Previous workers have shown that, in the case of plain sand over a non-ductile décollement, basin long-axis orientation depends on overburden thickness rela-



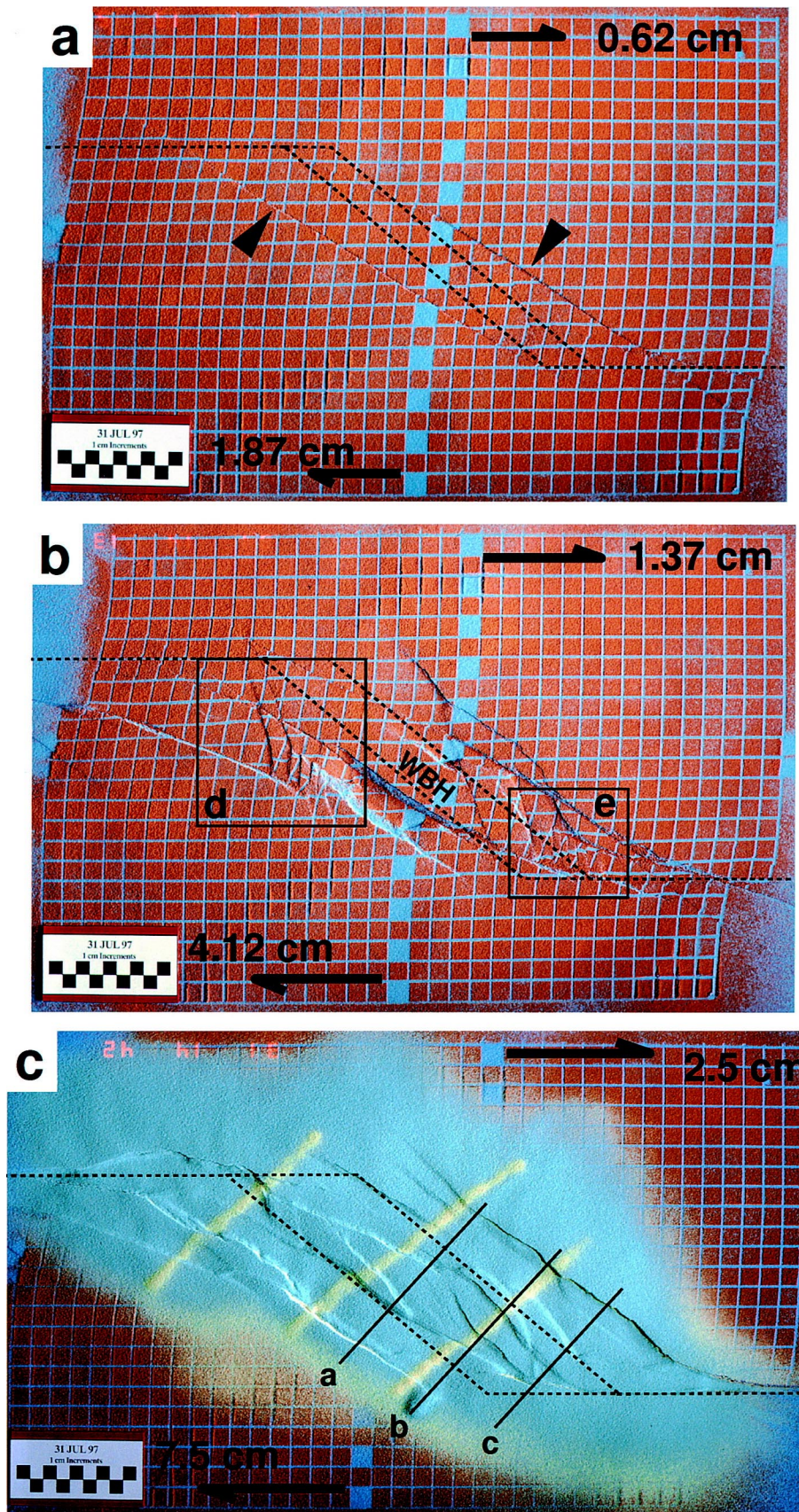


Fig. 5. Photographic map views showing pull-apart basin development over thin (0.5 cm) putty layer (Model 31Jul97). Black arrows in (a) mark sub-parallel **R** shears. Offset of yellow diagonal lines (c) show strike-slip displacement after application of last syn-kinematic growth layer. Thin solid lines marked a, b, and c show position of profile views in Fig. 8. In (d–e), enlarged views of areas outlined in (b) are shown. Details are the same as in Fig. 3.

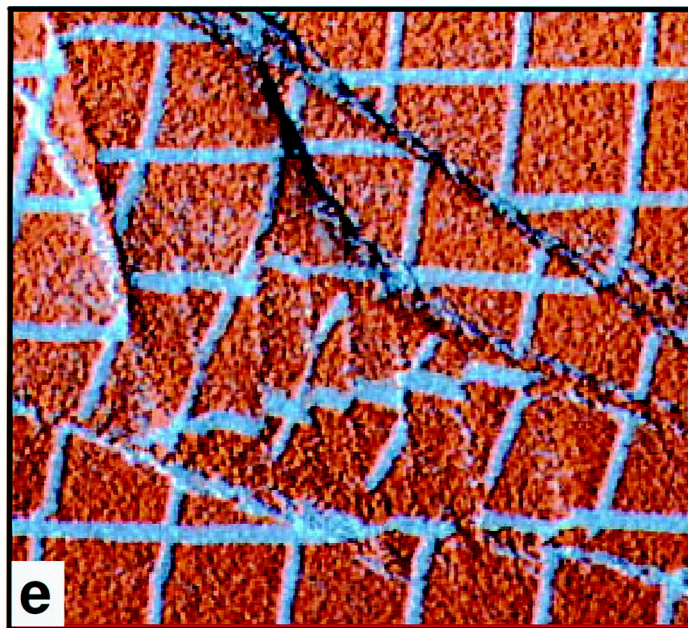


Fig. 5 (continued)

tive to strike-normal distance (step magnitude) between the primary strike-slip fault segments (**D**) in the mechanical décollement (plastic sheet in our models, see Fig. 1b; Mandl, 1988; Richard et al., 1995). Where overburden thickness is twice the step magnitude, basin axes parallel the step angle ( $40^\circ$  in our models). Basin axes are parallel with the primary strike-slip or **D** shears when overburden thickness is greater than the step magnitude (Mandl, 1988). With one exception (Model 9), the experiments presented here fall into the first category—step magnitude is more than twice the overburden thickness (Table 1). The orientation of the elongate basins produced in models with ductile décollements is in every case less

than (understates) the step angle and greater than zero (not parallel with the strike-slip faults in the plastic sheet).

### 3.1. Décollement thickness effect

Décollement (putty layer) thickness affects the spatial and kinematic distribution of major **R** shears in our models (Table 3). In thick (1 cm) décollement models, early forming **R** shears are subparallel, widely spaced, and numerous (Figs. 2 and 4). They develop later and remain active longer than in models with thin (0.5 cm) putty décollements (Figs. 5 and 6). Models with a 1-cm-thick décollement tend to form

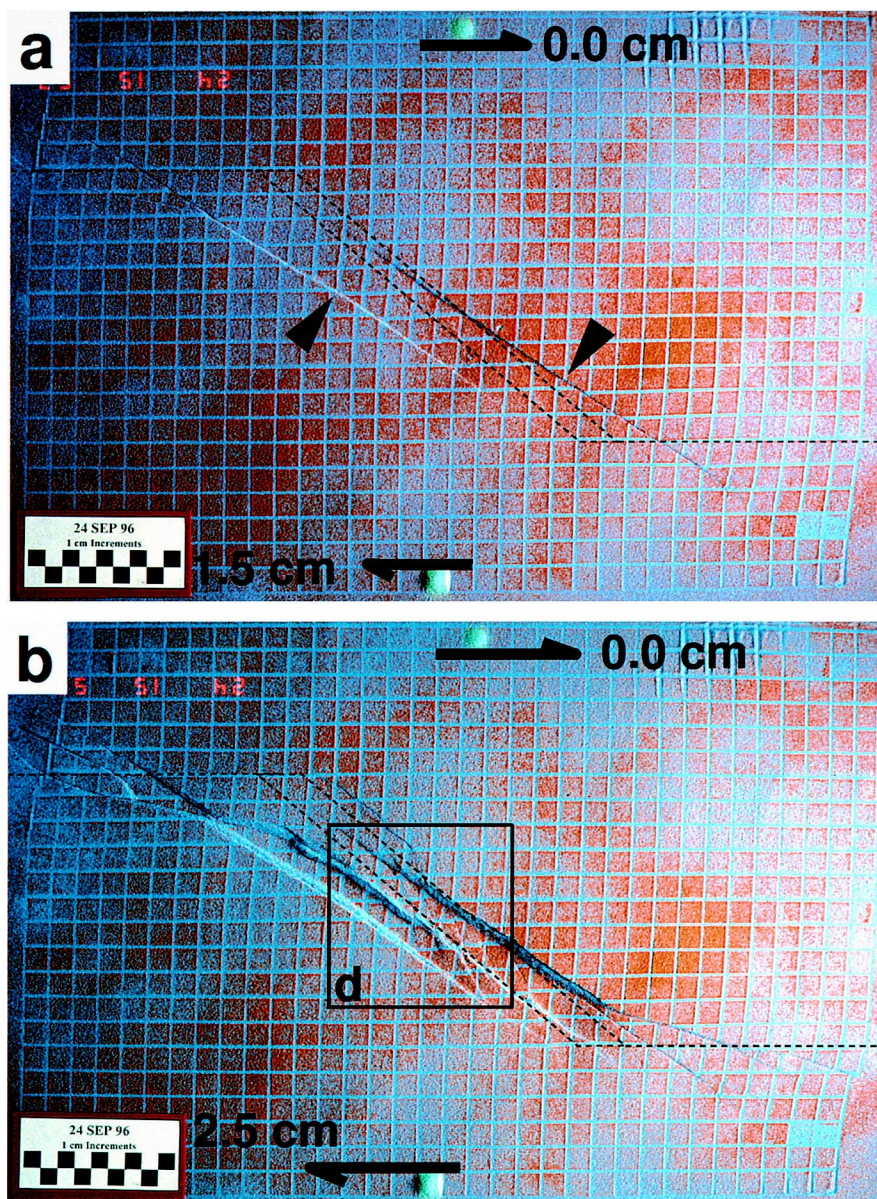


Fig. 6. Photographic map views showing pull-apart basin development over thin (0.5 cm) putty layer (Model 24Sep96). Black arrows in (a) mark sub-parallel **R** shears. Close up of duplexes in (b) are shown enlarged in (d). Details are the same as in Fig. 3.

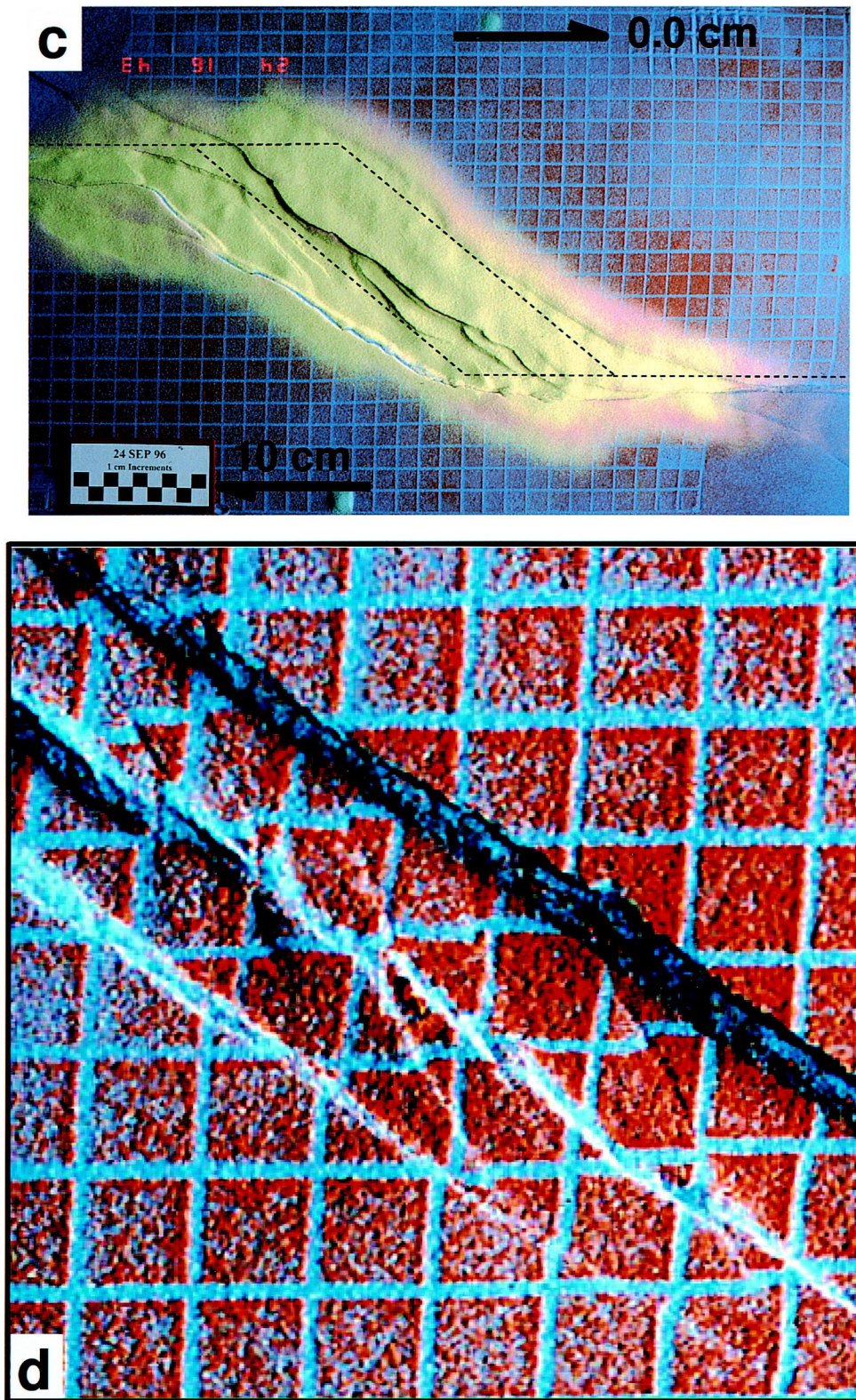


Fig. 6 (continued)

Table 3  
Structural features common to model décollement thickness

---

**Models with 1 cm thick ductile layer (silicone putty)**

---

Models 1, 2, and 3

- asymmetric basins form along major through-going strike-/oblique-slip shear flanked by widely-spaced, subparallel subsidiary strike-slip faults
  - later subsidence
  - elongate, narrow basins
  - isolated sub-basins (including trapdoor type) separated by between-basin highs
  - basin asymmetry reverses along strike of basin
  - basin asymmetry centered on through-going strike-slip fault
- 

**Models with 0.5 cm thick ductile layer (silicone putty)**

---

Models 4, 5, and 6

- asymmetric basins and sub-basins form between closely spaced subparallel strike-/oblique-slip shears
  - earlier subsidence
  - antithetic cross-basin faults create rotating duplexes between paired strike-slip faults
  - basin bisecting strike-slip faults
  - bisected strike-slip duplexes
  - coalescing sub-basins separated by within-basin highs produce wider basin complexes
  - basin asymmetry reverses along strike of basin
  - basin asymmetry centered along within-basin strike-slip transfer zones
- 

major basins that are elongate and narrow with widely spaced minor basins flanking the major basin. Major basin development is accommodated by localized normal faulting flanking a single through-going **R** shear (Fig. 4b). The through-going **R** shear in some cases becomes dormant as flanking **N** shears evolve to oblique-displacement faults (Figs. 4c and 7c). Subsidiary **R** shears commonly terminate at oblique-slip synthetic **R** and antithetic **R'** shears to form isolated trapdoor basins (Fig. 4c). Trapdoor basins form after the main basin begins to subside. Plan view basin orientation understates the right-stepping jog in the plastic sheet and subsidence begins later than in models with a thin (0.5 cm) putty base.

Models with 0.5 cm thick décollements tend to show earlier vertical displacement and produce basins that are subparallel with, but understate, the 40° step angle of the cut plastic sheet. Early formed subparallel **R** shears are linked by antithetic **R'** shears to form strike-slip duplexes (Figs. 2i, 5 and 6). Basin subsidence initiates when displacement on these **R** and linking **R'** shears evolves to oblique-slip (Figs. 5b and 6b). During the early stage of subsidence, a through-going **R** shear develops along the central basin axis that effectively bisects the basin footwall, including active duplexes, resulting in a complex footwall geometry (Fig. 6d). The bisecting **R** shears are in many cases long lived and locally accommodate normal displacement. Development of the basin-bisecting **R** shear subsides but does not terminate strike slip on the basin bounding faults or on the bisected duplexes. In some cases, duplex halves continue rotating after development of basin bisecting **R** shears. Models with thin ductile décollements also tend to produce basins that appear wider in plan view than those developed in

models with thick putty layers. In profile, the wider basins are composed of closely spaced sub-basins separated by footwall highs.

In profile view of the models with a 0.5 mm putty décollement, basin bounding master faults develop as steeply dipping **N** faults or as vertical to steeply dipping oblique-slip faults (**R** shears). Hanging wall roll-over is commonly toward the active **R** shear (Figs. 7 and 8). Major **R** shears show convex or concave profiles near strike-slip transfer zones or where the shear has a late developing normal slip component. **R** shears with no normal slip component are vertical or subvertical with no apparent offset in profile view. These faults are identified in profile by a dilatant zone in the sandpack (Figs. 7 and 9a) and by offset of the passive grid in plan view.

Basin asymmetry is controlled by the geometry of **R** shears. In our models, the geometry of **R** shears is controlled by putty layer thickness. End member cases are asymmetrically developed along a single through-going **R** shear or, in the absence of a through-going shear, asymmetrically developed between subparallel **R** shears. In the thick-décollement (1.0 cm) models, basin asymmetry commonly centers along a dominant **R** shear with the central basin axis switching from one to the other side along strike (Fig. 7, Table 3). Ductile pull-aparts that develop between subparallel en échelon **R** shears in thin décollement (0.5 cm) models (Figs. 5 and 6) show asymmetry centered along within-basin strike-slip transfer zones. Strike-slip transfer zones are marked by between- or within-basin highs in the pre-kinematic layers (Figs. 7–9). In plan view, the highs are elongate and subparallel to the basin margins and separate the deeper opposing ends of the elongate basins (Fig. 6b).

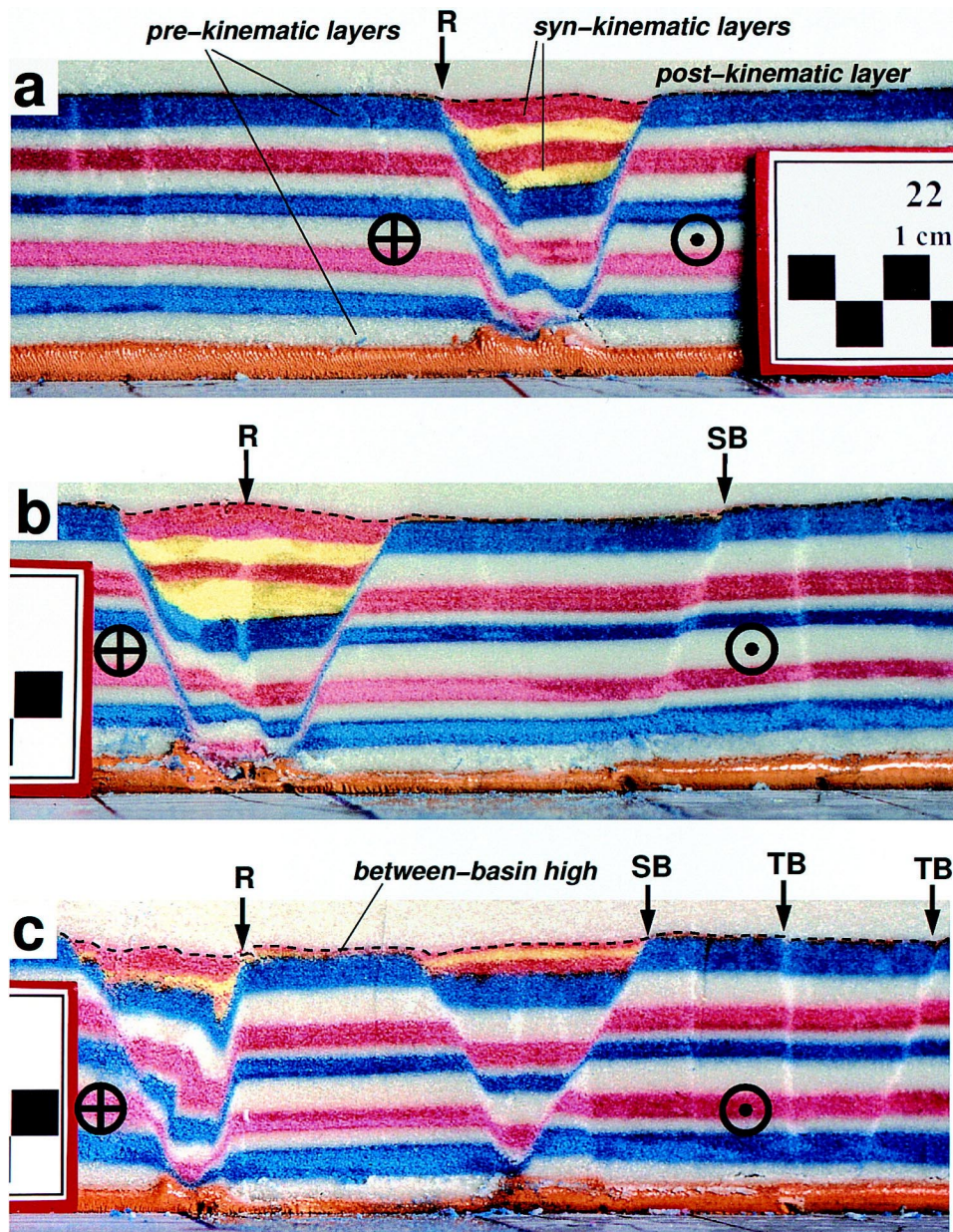


Fig. 7. Profile views of pull-apart basin developed over 1 cm thick putty layer (Model 1). Black arrows (R) mark early-forming R shear. SB marks sub-basin master fault. Light colored vertical and dipping streaks in (c), marked by arrows TB, are strike- and oblique-slip faults at the margin (hinge) of an isolated trapdoor basin. Details are the same as in Fig. 3.

### 3.2. Velocity effect

Rahe et al. (1998) demonstrated that velocity differences across the primary strike-slip faults affect basin symmetry, where basin symmetry is defined by the location of normal or oblique-slip master faults. In cases in which opposing blocks (Figs. 1b and 3) move at equal and opposite rates, basins are approximately symmetrical with some opposing asymmetry at basin ends. In cases in which opposing blocks move at different opposing rates, the resulting basins are asymmetrical and the degree of basin asymmetry increases with the difference in rate between the opposing blocks. The

greatest degree of asymmetry is observed where one block is stationary relative to the opposing block (Fig. 1b). In our putty décollement models, relative rate effects are subdued by the mobile décollement. Each run produced basins with some degree of asymmetry that varied along strike (Figs. 7–9). The degree of asymmetry increases with differences in relative velocity magnitude, with the axis of maximum vertical displacement located nearer the faster moving décollement. The tendency for basin asymmetry to reverse along strike is less pronounced where relative displacement ratios are large (10:0) and putty thickness is small (0.5 cm).

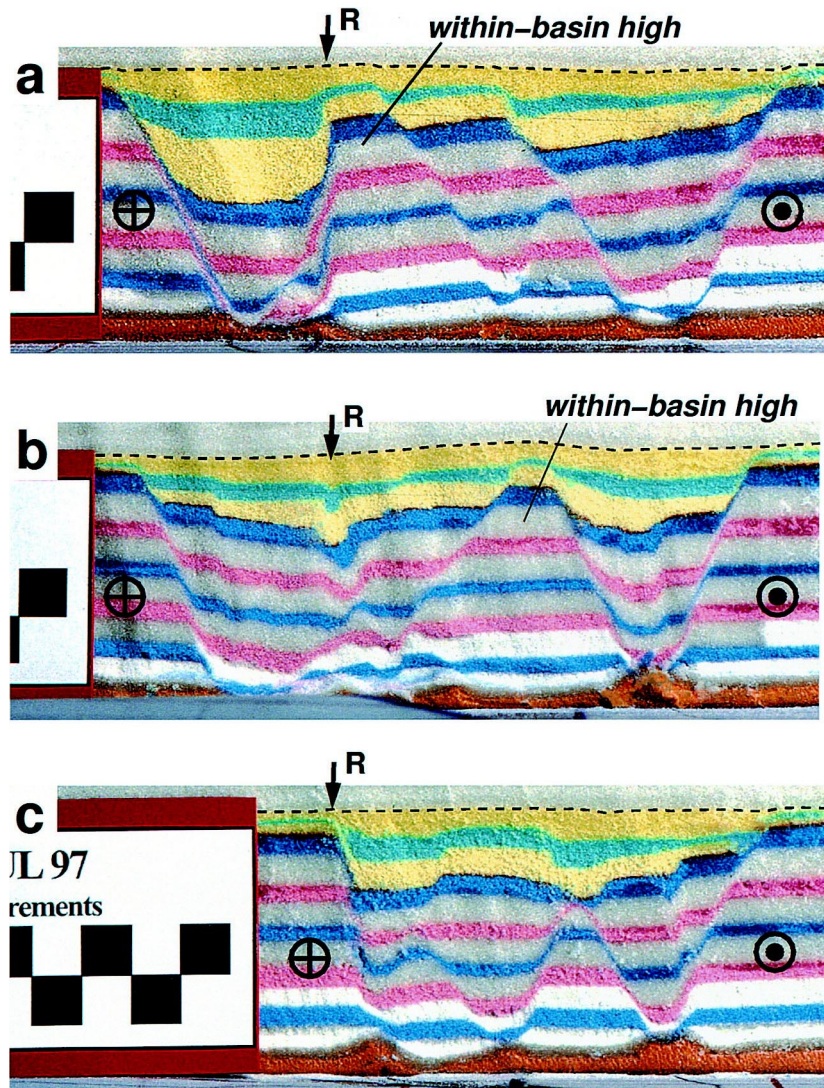


Fig. 8. Profile views of pull-apart basin developed over 0.5 cm thick putty layer (Model 5). Within-basin strike-slip transfer zone marked by arrows (R). Details are the same as in Fig. 3.

### 3.3. Absolute rate effect

To test the effects of rate control upon pull-apart development over a viscous substrate, a single model (24Jul97) was constructed to emulate faster slip rates. All physical parameters are identical except for an order of magnitude increase in putty viscosity (Table 2) effectively changing the representative model velocities by one order of magnitude. Putty thickness is 1 cm and displacement velocity is 1:1 where opposing sides move at 5 cm/h for one hour (Table 1). Results are similar to those from slower rate models, with some exceptions: isolated sub-basins did not appear and basin trend is closer to, but still subparallel with, the 40° step in the plastic décollement. Sub-basins were closely spaced, asymmetric, and separated by a subparallel within-basin high similar to 0.5 cm thick putty models. Although basin asymmetry did not clearly

reverse, the locus of maximum subsidence did switch sides along strike.

### 3.4. Step magnitude

A preliminary series of experiments designed to test boundary conditions and explore variables in model design included model 26Jul96 (Table 1, Fig. 10). The setup is identical to 1-cm-thick putty models with the exception of step magnitude and direction and model scaling (Table 2). The 10 cm magnitude step is to the left and the model is scaled to represent a weaker, less dense décollement at shallower depth than the remainder of the series (Tables 1 and 2). Similar to 1-cm-thick putty layer models with larger step magnitude, the model presents a through-going strike-slip fault, or **R'** shear, with a normal-slip component that varies along strike. Basin asymmetry is into the major strike-

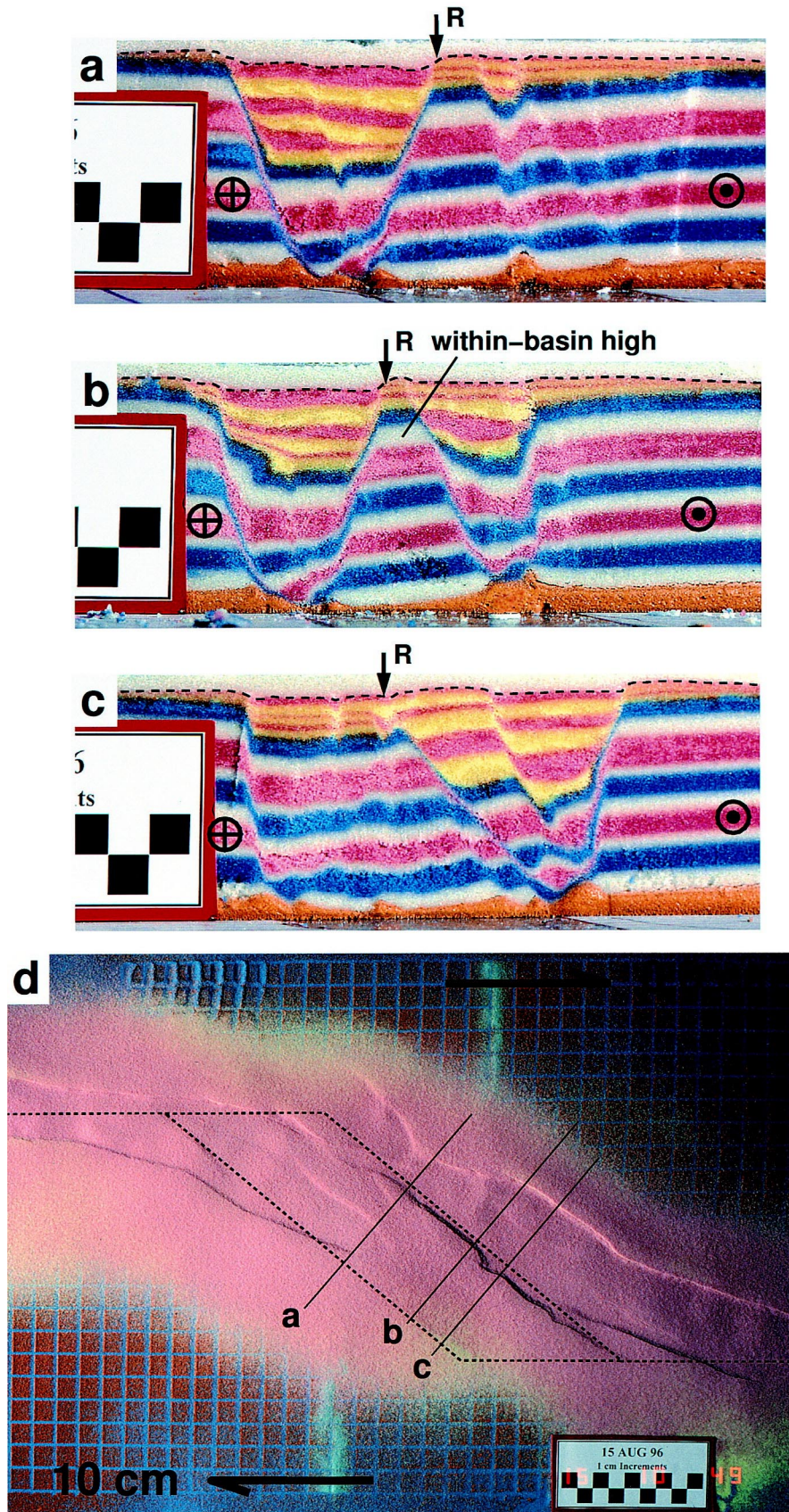


Fig. 9. Profile views of pull-apart basin developed over 1 cm thick putty layer (Model 3). Reversal of asymmetry along strike of same fault (arrows R) and across within-basin high is shown. The basin axis moves from updip (c) to downdip (a) along strike. Post-kinematic map view of model 3 is shown in (d). Location of profile views (a–c) shown by thin solid line.



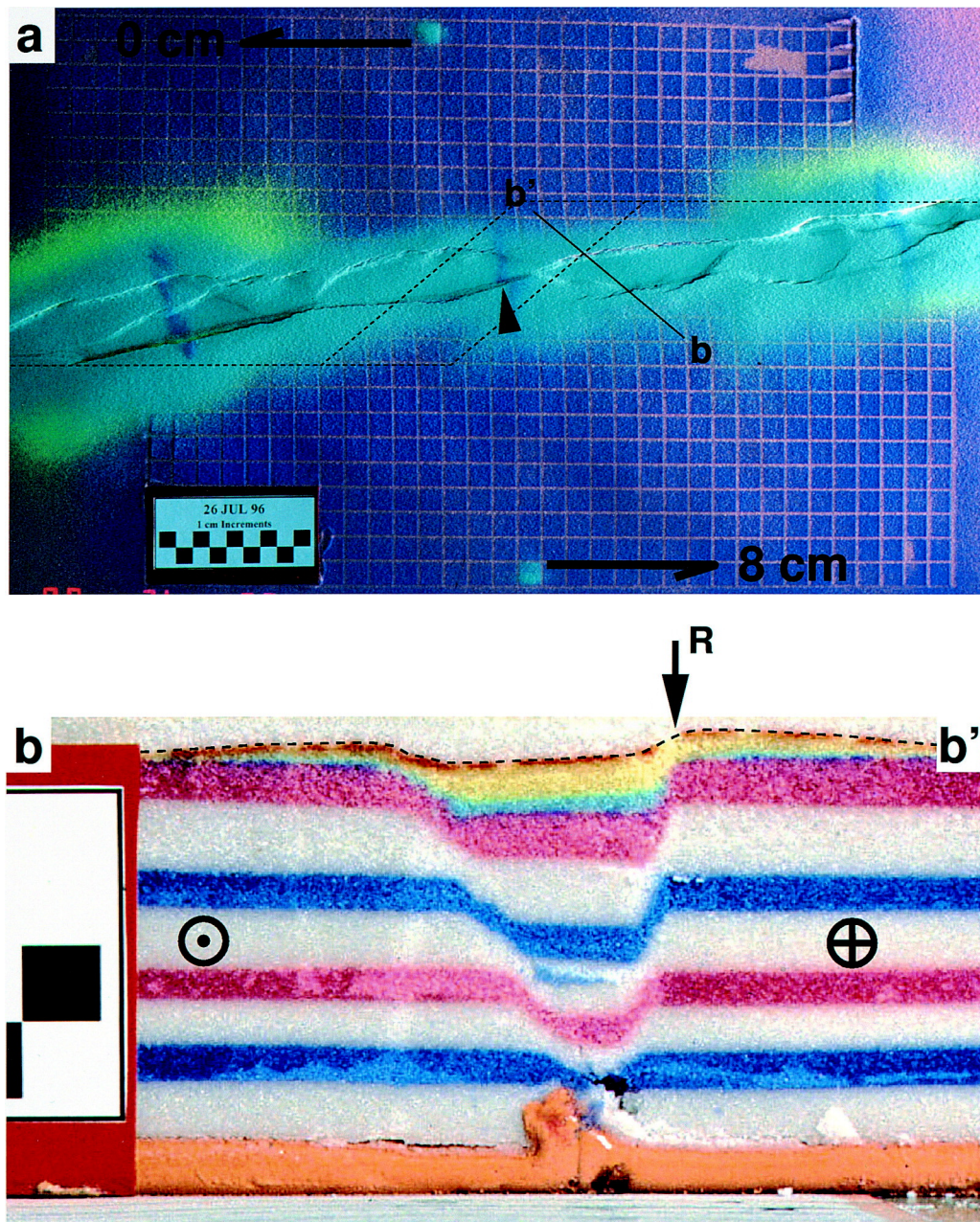


Fig. 10. (a) Photographic map view of smaller step-normal maghear. Fig. 1(b), all other details are the same as in Fig. 3. Asymmetric sub-basins (a) distributed along a through-going **R** shear show undulating surface with localized lows. Left-stepping jog of through-going **R** shear in (a) is marked with black arrow. Symmetry reverses along strike from that shown in (b) to opposing symmetry to the left of the black arrow. In (b), heavy black arrow (**R**) shows location of through-going **R** shear.

slip fault and reverses along strike; minor basin bounding faults show normal and strike-slip displacements.

#### 4. Discussion

Physical models of pull-apart basins over ductile décollements produced in this study are characterized by a system of subparallel, elongate, and narrow asym-

metric basins. Strike-slip faulting precedes normal and oblique-slip faulting and strike-slip motion continues throughout the duration of the experiments. Basin asymmetry tends to reverse along strike, separating main basins into along-strike sub-basins. Subparallel sub-basins may be closely spaced and coalesce to appear as a single large basin in plan view or widely spaced, with later-forming isolated minor basins flanking the major basins. These processes are similar to the

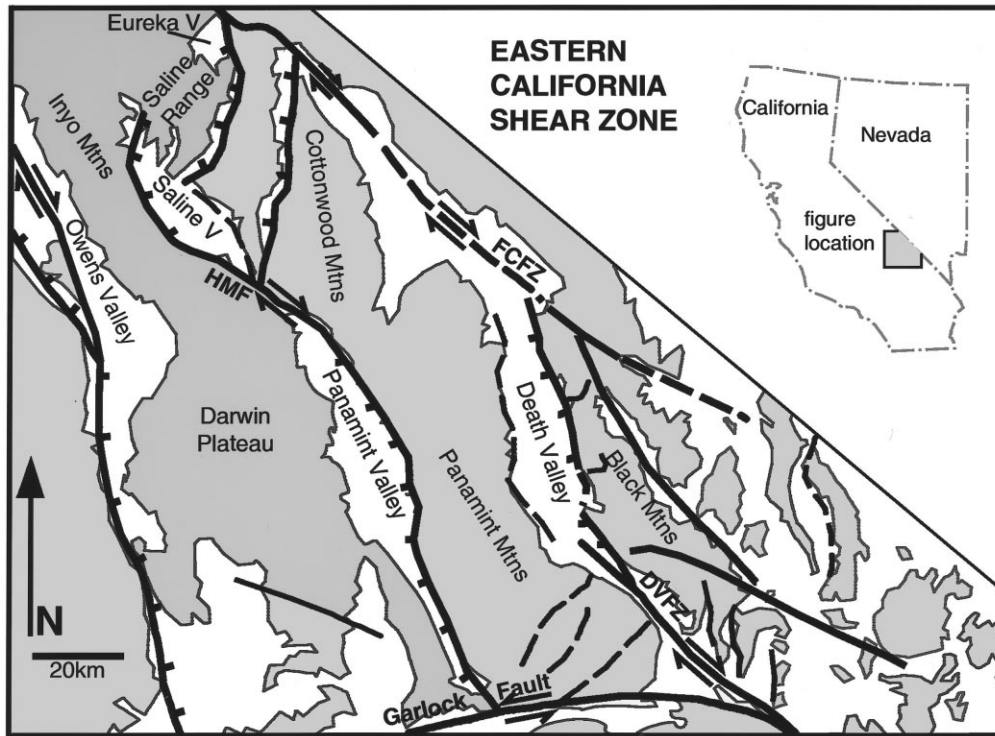


Fig. 11. Generalized structure map of the eastern California Shear Zone. White areas show extent of basin fill. FCFZ—Furnace Creek Fault Zone, DVFZ—Death Valley Fault Zone, HMF—Hunter Mountain Fault. Modified from Burchfiel et al. (1987).

models for pull-apart development proposed by Aydin and Nur (1982), where closely spaced en échelon basins or widely spaced later-forming basins coalesce to form composite pull-apart basins.

Basin footwall geometries often appear deceptively simple in profile, but are born of kinematic complexities. Structures that appear as normal faults in basin hanging walls may be oblique-slip antithetic  $R'$  shears defining rotated fault-bounded horses (Figs. 8c and 9c). Some antithetic cross-basin faults are active throughout basin development (Fig. 5) with some downdropped and rotated duplexes marking the deepest points in the basins. Where duplexes are bisected by later forming through-basin  $R$  shears, the opposing rotated and translated duplexes or duplex halves may have different subsidence histories.

#### 4.1. Eastern California shear zone

Plan view orientation and distribution of basins in our models show a remarkable similarity with composite pull-aparts observed in nature. The eastern California shear zone, including Owens, Eureka, Saline, Panamint, Fish Lake, and Death Valleys is a system of strike-slip and normal dip-slip faults that interconnect to form a right-lateral system of pull-apart basins of varying geometries (Fig. 11). While in-

dividual basin geometries and kinematics are still the subject of debate (Reheis et al., 1993; Dixon et al., 1995; Serpa and Pavlis, 1996), the distribution of sub-basins is similar to the pattern produced in our models. Owens, Panamint, Eureka, Saline, Fish Lake, and Central Death Valleys are subparallel and separated by subparallel within-basin highs. While it is not clear that each valley is formed above a deep décollement (Burchfiel et al., 1987), the eastern California shear zone has been interpreted to form above a décollement in the ductile lower crust (Burchfiel et al., 1989). Our models demonstrate that such systems develop where releasing bends evolve over a ductile décollement.

#### 4.2. Gulf of Elat, Dead Sea Rift

The Gulf of Elat (Aqaba), southern Dead Sea Rift, is a pull-apart system along the left-slip African–Arabian plate boundary. The system is bathymetrically and structurally divided into elongate, narrow, en échelon sub-basins of varying depth including, from north to south, Elat, Aragonese, Arnona, Dakar, and Tiran Deep (Fig. 12). Basins are asymmetric in profile and bound by longitudinal subparallel opposing strike-slip and normal-slip faults (Ben-Avraham and Zoback, 1992), with basin asymmetry into the strike-slip fault

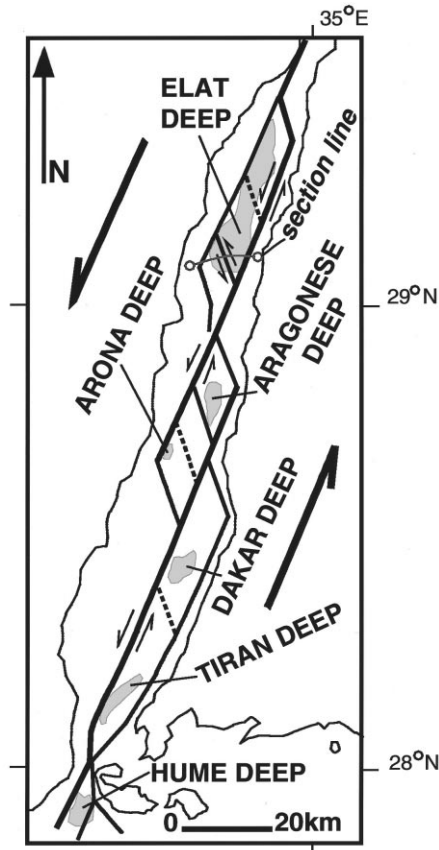


Fig. 12. Generalized structure map of the Gulf of Elat, southern Dead Sea Rift modified from Ben-Avraham and Zoback (1992). Shaded areas show bathymetric 'deeps.'

(Fig. 13). Sub-basins are terminated or transected by transverse strike- and normal-slip faults. Subhorizontal to gentle dip of basin fill indicates a normal-slip component along some strike-slip faults and basin asymmetry reverses along strike of the pull-apart zone. Most décollements are in evaporites (ten Brink and Ben-Avraham, 1989).

Basin topology and geometry of 1-cm-thick putty décollement models resemble those of the Gulf of Elat. Basins are numerous, elongate, narrow, asymmetric, and bound by strike- and oblique-slip faults. Basin symmetry reverses along strike. Basins in the Gulf of Elat are not widely spaced, as predicted by our models, and the system is not interpreted as forming about a single through-going strike-slip fault. Rather, basins are arranged en échelon along the pull-apart zone. The physical setting of the Gulf of Elat is not directly reflected in our large step-magnitude (16.2 cm) analogue models: offset of the primary strike-slip fault segments (step magnitude) in our models is greater than that observed in the Gulf of Elat and décollement strength in these models is scaled to represent the duc-

tile crust, not a weaker material such as the décollements in salt present in the Gulf of Elat.

Model 9 (Table 1), scaled to represent a less-dense and less-viscous basal layer with a smaller step magnitude (10 cm), closely reflects the fault patterns and basin distribution in the Gulf of Elat (Figs. 10, 12 and 13). Map trace of the through-going strike-slip fault in the model shows somewhat angular jogs or bends, particularly in the center of the basin complex where basin asymmetry is observed to switch sides. This geometry is similar to that surrounding the Aragonese Deep (Fig. 12), where transverse faults are interpreted as linking separate linear, sub-parallel, and en échelon strike-slip basin-bounding faults. Results from physical models suggest that the strike-slip faults flanking the Aragonese Deep are joined by a dominant transverse fault to form a continuous strike-slip system. Though basin asymmetry reverses along strike of both the natural and analogue pull-apart basins, the sense of asymmetry is reversed. This opposing symmetry sense between natural example and analogue may be related to the corresponding difference in kinematics. While this model shows a strong resemblance to the Gulf of Elat pull-apart basin system, the experiment was designed to emulate a simple pull-apart system. The Gulf of Elat pull-apart is reported as having a slight component of opening (Ben-Avraham, 1985; after Le Pichon and Francheteau, 1978), while our models are

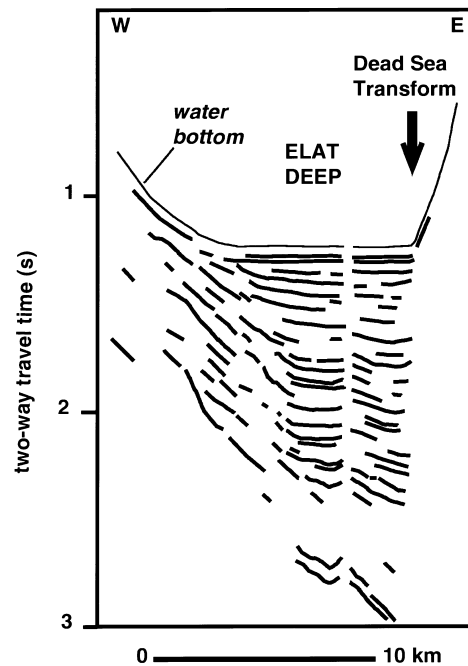


Fig. 13. Line drawing of asymmetric basin in Dead Sea Rift from seismic data (after Ben-Avraham and Zoback, 1992). Vertical axis is two-way travel time. Heavy arrow shows location of Dead Sea Transform. See Fig. 12 for location.

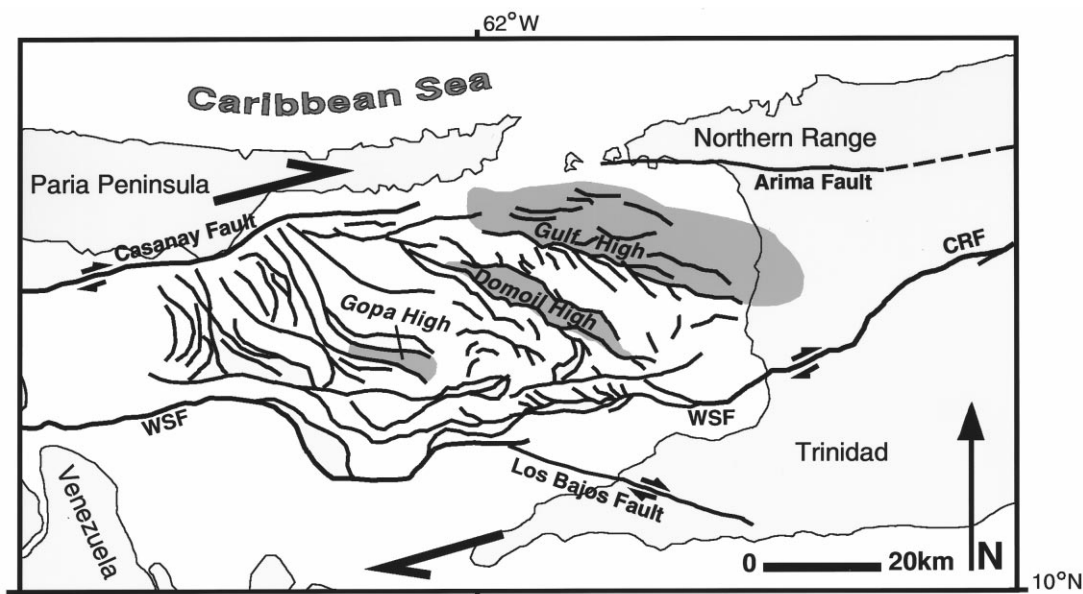


Fig. 14. Generalized map of the Gulf of Paria, northeastern Venezuela showing major structures of pull-apart basin complex modified from Flinch et al. (in press). Casanay, Los Bajos, Warm Springs (WSF), and Central Range Faults (CRF) are strike-slip shears at basin ends. Gopa, Gulf, and Domoil inter-basin highs (dark shading) separate subparallel asymmetric basins.

restricted to pure strike-slip motion along the mechanical décollement. In addition, the mechanical décollement in the model represents a single pair of en échelon basement faults. Basement geometry in the Gulf of Elat is unlikely to be as simple.

#### 4.3. Gulf of Paria, eastern Venezuela and Trinidad

The Gulf of Paria (Venezuela and Trinidad) pull-apart basin is a right-lateral, right-stepping, composite pull-apart system along the South Caribbean Plate Boundary (Harding and Tuminas, 1989; Algar and Pindell, 1993; Avé Lallement, 1997; Flinch et al., in press). This system is composed of asymmetric sub-basins separated by subparallel within-basin highs (Domoil and Gopa) (Fig. 14). Basin asymmetry switches sides along strike of basins arrayed between and terminated by the Warm Springs and Casanay strike-slip faults. Décollements are in shales or evaporites (Flinch et al., in press). Recent workers compared the Gulf of Paria pull-apart basin to analogue models of pull-aparts (Flinch et al., in press) where the models do not employ a ductile substrate. One distinct contrast between the Gulf of Paria and plain sandpack models is that the system of sub-basins separated by within-basin highs present in the Gulf of Paria pull-apart (Fig. 14) is not reproduced in sandpack-only physical models. Distribution of sub-basins and highs more closely resembles the pattern produced by the thin-putty-layer based models presented here.

Longitudinal basin-bounding faults in the Gulf of Paria show orientations similar to the basin-bounding **R** shears produced in our ductile substrate models, suggesting that at least some of the longitudinal basin-bounding normal faults in the Gulf of Paria have a significant strike-slip component. Faults mapped by Flinch et al. (in press) in the basin hanging wall between the Gulf and Domoil Highs show an orientation similar to the antithetic cross-basin faults (**R'** shears) produced in the thin-layer putty-based models (Fig. 14). In the models, these faults link with the basin-bounding faults to form strike-slip duplexes. This system of duplexes is sometimes transected by a longitudinal strike-slip fault situated along the basin axis (Fig. 6d) resulting in decreased normal slip on some antithetic cross-basin fault segments, with increased activity on other segments. The fault traces as mapped by Flinch et al. (in press) do not extend across the basin, but terminate near the basin central axis. This pattern is expected where the antithetic cross-basin faults have been transected by a strike-slip fault along the basin axis. These transecting strike-slip faults are sometimes difficult to detect in the physical models, especially where there is little or no vertical slip component. Pre-kinematic layers in the hanging wall may show no offset. Syn-kinematic or 'basin fill' layers may show no thickness change across the axially centered strike-slip fault where antithetic cross-basin faults experience zero or identical vertical displacement. Localized normal slip on some antithetic cross-

basin fault segments may produce abrupt thickness change across the central strike-slip fault. This scenario would be particularly difficult to detect in seismic data where reflectors from similar lithologies appear continuous across the fault zone and may be indicated where abrupt thickness, lateral sequence, or facies changes are observed.

## 5. Conclusions

The occurrence of pull-apart systems with strike-slip dominated asymmetric basins present facets of basin development, geometry, and kinematics that cannot be explained by traditional conceptual models (Carey, 1958; Burchfiel and Stewart, 1966) of pull-apart basins. Natural examples, including the Gulf of Elat (Aqaba), Gulf of Paria (Venezuela and Trinidad), and the Cariaco Basin (northern Venezuela) indicate that depth-to-décollement, décollement rheology, or both are controlling factors in basin morphology.

Experimental results and natural examples indicate that décollement zone strength and thickness controls pull-apart basin development and geometry. Pull-apart depressions dominated by a single basin with dominant normal-slip master faults result from strong décollement zones. Depressions comprised of complexes of isolated or coalescing sub-basins having strike-slip dominated geometries are more characteristic of weak décollement zones.

Décollement zone strength affects basin symmetry by subduing the effects of relative displacement. Symmetry in pull-apart basins developed over strong décollement zones is controlled by relative displacement of the opposing basin walls. Symmetry in the case of strong décollements varies from symmetric in the case of equal displacement of opposing walls to asymmetric in the case of disparate displacement of opposing basin walls (Rahe et al., 1998). Basins or basin complexes with weak décollement zones are markedly asymmetric regardless of relative displacement rates, with asymmetry commonly reversing along strike of the pull-apart zone. Development of through-going cross-basin faults mark the mature development stage of pull-apart systems with strong décollements (Rahe et al., 1998) and may result in a marked decrease in basin subsidence. In contrast, strike-slip faults evolve early and are long lived where décollement zone strength is low, and control the locus of basin subsidence.

## Acknowledgements

This report documents analyses performed by the Center for Nuclear Waste Regulatory Analyses

(CNWRA) for the Nuclear Regulatory Commission (NRC) under contract numbers NRC-02-93-005 and NRC-02-97-009. This paper is an independent product of the CNWRA and does not necessarily reflect the views or regulatory positions of the NRC. We thank Barbara Long for editorial review, Annette D. Mandujano for assistance in manuscript preparation, and Lena Krutikov and Michael Ferguson for assistance with figure preparation. We also thank H. Lawrence McKague, Wesley C. Patrick, L.B. Harris, Sean Willett, Don Fisher, and an anonymous reviewer for comments that greatly improved the manuscript.

## References

- Algar, S.T., Pindell, J.L., 1993. Structure and deformation history of the Northern Range of Trinidad and adjacent areas. *Tectonics* 12, 814–829.
- Avé Lallement, H.G., 1997. Transpression, displacement partitioning, and exhumation in the eastern Caribbean/South American plate boundary zone. *Tectonics* 16, 272–289.
- Aydin, A., Nur, A., 1982. Evolution of pull-apart basins and their scale independence. *Tectonics* 1, 91–105.
- Aydin, A., Nur, A., 1985. The types and role of stepovers in strike-slip tectonics. In: Biddle, K., Christie-Blick, N. (Eds.), *Strike-slip Deformation, Basin Formation, and Sedimentation*, Society of Economic Paleontologists and Mineralogists, Special Publication, 37, pp. 35–44.
- Ben-Avraham, Z., 1985. Structural framework of the Gulf of Elat (Aqaba), Northern Red Sea. *Journal of Geophysical Research* 90, 703–726.
- Ben-Avraham, Z., 1992. Development of asymmetric basins along continental transform faults. *Tectonophysics* 215, 209–220.
- Ben-Avraham, Z., Zoback, M., 1992. Transform-normal extension and asymmetric basins: An alternative to pull-apart models. *Geology* 20, 423–426.
- Burchfiel, B., Stewart, J., 1966. 'Pull-apart' origin of the central segment of Death Valley, California. *Geological Society of America Bulletin* 77, 439–442.
- Burchfiel, B.C., Hodges, K.V., Royden, L.H., 1987. Geology of Panamint Valley–Saline Valley pull-apart system, California: Palinspastic evidence for low-angle geometry of a Neogene range-bounding fault. *Journal of Geophysical Research* 92, 10422–10426.
- Burchfiel, B.C., Quidog, D., Molnar, P., Royden, L., Yipneg, W., Peizhen, Z., Weiqui, Z., 1989. Intracrustal detachment within zones of continental deformation. *Geology* 17, 448–452.
- Carey, S., 1958. The tectonic approach to continental drift. In: *Continental Drift, A Symposium*. Geology Department, University of Tasmania, Hobart.
- Cloos, E., 1955. Experimental analysis of fracture patterns. *Geological Society of America Bulletin* 66, 241–256.
- Dixon, T.H., Robaudo, S., Lee, J., Reheis, M., 1995. Constraints on present-day basin and range deformation from space geodesy. *Tectonics* 14, 755–772.
- Faugère, E., Brun, J., van den Driessche, J., 1986. Bassins asymétriques en extension pure et en décrochement: Modèles expérimentaux. Asymmetric basins in pure extension and in wrenching: Experimental models. *Bulletin des Centres de Recherches Exploration–Production Elf-Aquitaine* 10, 13–21.
- Flinch, J., Rambaran, V., Ali, W., De Lisa, V., Hernandez, G., Rodrigues, K., Sams, R., 1998. Structure of the Gulf of Paria Pull-Apart Basin (Eastern Venezuela–Trinidad). In: Mann, P.

- (Ed.), *Caribbean Sedimentary Basins*, Elsevier Basins of the World. Elsevier, Amsterdam.
- Harding, T.P., Tuminas, A.C., 1989. Structural interpretation of hydrocarbon traps sealed by basement normal block faults at stable flank of foredeep basins and at rift basins. *American Association of Petroleum Geologists Bulletin* 73, 812–840.
- Hempton, M., Neher, K., 1986. Experimental fracture, strain and subsidence patterns over an échelon strike-slip faults: Implications for the structural evolution of pull-apart basins. *Journal of Structural Geology* 8, 597–605.
- Hubbert, M.K., 1937. Theory of scale models as applied to the study of geologic structures. *Geological Society of America Bulletin* 48, 1459–1520.
- Jackon, J.A., 1997. *Glossary of Geology*, 4th ed. American Geological Institute, Alexandria, Virginia.
- Le Pichon, X., Francheteau, J., 1978. A plate-tectonic analysis of the Red Sea–Gulf of Aden area. *Tectonophysics* 46, 369–406.
- Mandl, G., 1988. *Mechanics of Tectonic Faulting, Models and Basic Concepts*. Elsevier, Amsterdam.
- McClay, K., Dooley, T., 1995. Analogue models of pull-apart basins. *Geology* 23, 711–714.
- McClay, K., Ellis, P., 1987. Analogue models of extensional fault geometries. In: Coward, M., Dewey, J., Hancock, P. (Eds.), *Continental Extensional Tectonics*, Geological Society, Special Publication, 28, pp. 109–125.
- Molnar, P., Lyon-Caen, H., 1988. Some simple physical aspects of the support, structure, and evolution of mountain belts. In: Clark Jr., S.P., Burchfiel, B.C., Suppe, J. (Eds.), *Processes in Continental Lithospheric Deformation*. Geological Society of America, Special Paper 218.
- Price, N., Cosgrove, J., 1990. *Analysis of Geological Structures*. Cambridge University Press, Cambridge.
- Rahe, B., Ferrill, D., Morris, A., 1998. Physical analog modelling of pull-apart basin evolution. *Tectonophysics* 285, 21–40.
- Ramberg, H., 1967. *Gravity, Deformation, and the Earth's Crust as Studied by Centrifuge Models*. Academic Press, New York.
- Reheis, M.C., Slate, J.L., Sarna-Wojcicki, A.M., Meyer, C.E., 1993. A late Pliocene to middle Pleistocene pluvial lake in Fish Lake Valley, Nevada and California. *Geological Society of America Bulletin* 105, 953–967.
- Richard, P., Mocquet, B., Cobbold, P., 1991. Experiments on simultaneous faulting and folding above a basement wrench fault. *Tectonophysics* 188, 133–141.
- Richard, P.D., Naylor, M.A., Koopman, A., 1995. Experimental models of strike-slip tectonics. *Petroleum Geoscience* 1, 71–80.
- Schubert, C., 1984. Basin formation along the Bocono–Moron–El Pilar fault system, Venezuela. *Journal of Geophysical Research* 89, 5711–5718.
- Serpa, L., Pavlis, T.L., 1996. Three-dimensional model of the late Cenozoic history of the Death Valley region, southeastern California. *Tectonics* 15, 1113–1128.
- Tchalenko, J., 1970. Similarities between shear zones of different magnitudes. *Geological Society of America Bulletin* 81, 1625–1640.
- ten Brink, U., Ben-Avraham, Z., 1989. The anatomy of a pull-apart basin: Seismic reflection observations of the Dead Sea Basin. *Tectonics* 8, 333–350.
- Vendeville, B., Cobbold, P., Davy, P., Brun, J., Choukroune, P., 1987. Physical models of extensional tectonics at various scales. In: Coward, M., Dewey, J., Hancock, P. (Eds.), *Continental Extensional Tectonics*, Geological Society, Special Publication, 28, pp. 95–107.
- Withjack, M., Islam, Q., LaPoint, P., 1995. Normal faults and their hangingwall deformation: An experimental study. *American Association of Petroleum Geologists Bulletin* 79, 1–18.
- Zhang, P., Burchfiel, B.C., 1989. Extinction of pull-apart basins. *Geology* 17, 814–817.